THE EFFECT OF GEL VOLUME IN AUTOCLAVE ON THE SYNTHESIS OF MORDENITE FROM RICE HUSK SILICA BY HYDROTHERMAL METHOD

Suriyan Rakmae and Jatuporn Wittayakun*

Received date: November 16, 2014 Revised date: February 14, 2015 Accepted date: February 16, 2015

Abstract

Two types of rice husk silica (RHS) were used in hydrothermal syntheses of mordenite in sodium form (NaMOR). Acid treated RHS was prepared by refluxing rice husk with hydrochloric acid followed by calcination. Precipitated rice husk ash (RHA) was prepared by dissolution of RHA in sodium hydroxide solution followed by precipitation. The synthesis gel volume was 30, 50, and 70% of that of a Teflon-lined stainless steel autoclave. The NaMOR products from both silica sources were analyzed by X-ray diffraction (XRD), X-ray fluorescence, N_2 adsorption-desorption analysis, ammonia temperature programmed desorption, and scanning electron microscopy. All samples showed characteristic XRD peaks of the NaMOR. The properties of the products including the Si/Al ratio, surface area, acidity, and morphology were influenced by the gel volume in the autoclave and the silica sources.

Keywords: Mordenite, hydrothermal synthesis, rice husk silica, reflux, precipitation

Introduction

In several countries, including Thailand, rice husk (RH) is produced in large quantities as a byproduct from rice milling. RH is composed of about 20 wt% of inorganic compound with silica as a main component (about 85-98% wt%) and trace metallic element impurities (Juliano *et al.,* 1987). Silica from RH has a uniform dispersion by molecular units, and a fine amorphous particle size with a high purity and surface area (Liou *et al*., 2011). There are several methods to obtain silica with high purity from RH. Acid treated rice husk silica (RHS) was prepared by refluxing RH with an acid followed by calcination (Liou, 2004; Panpa and Jinawath, 2009; Krishnarao *et al*., 2001). Another method employed rice husk ash (RHA), which was obtained by burning the RH which has a silica purity of 76-95 wt% (Kordatos *et al*., 2008; Naskar *et al*., 2012; Tepamat *et al*., 2013). Precipitated RHA was prepared by dissolution of RHA in a NaOH solution followed by precipitation with an acidic solution (Kalapathy *et al*., 2000).

With high purity, RHS can be used as

School of Chemistry, Institute of Science, Suranaree University of Technology, Nakhon Ratchasima 30000, Thailand. Tel.: +66 44 224 256; fax: +66 44 224 185. E-mail: jatuporn@sut.ac.th

* *Corresponding authorr*

a silica source for the production of porous inorganic materials such as zeolites LSX (Khemthong *et al*., 2007), NaY (Wittayakun *et al*., 2008; Khabuanchalad *et al*., 2008), NaBEA (Loiha *et al*., 2009), NaZSM-5 (Pimsuta *et al*., 2012), and MCM-41 mesoporous silica (Artkla *et al*., 2008). Moreover, RH charcoal was used as a silica source for the synthesis of zeolite NaA (Tepamat *et al*., 2013) and silicon carbide (SiC) (Makornpan *et al*., 2013). The interest of this work was to use acid treated RHS and precipitated RHA for the synthesis of zeolite mordenite (MOR).

MOR is a zeolite with interconnected pore channels between 12-membered ring and 8-membered ring openings (Baerlocher and McCusker, 2007). The unit cell dimensions of NaMOR were first reported by Meier (1961). It has a pore channel between a 12-membered ring in the c-axis and an 8-membered ring in the b-axis. The Si/Al ratio of MOR can be varied depending on the composition of the synthetic batch (Roland and Kleinschmit, 2003). MOR has been used as a solid catalyst for various industrial chemical reactions (Pantu *et al*., 2007).

Kulawong *et al*. (2011) reported a synthesis of NaMOR in sodium form (NaMOR) using RHS. They crystallized the NaMOR in a Teflon-lined autoclave with a 150 mL capacity at various times and used the optimal condition for a synthesis with another autoclave with a 250 mL capacity. However, the void volume was not reported for both vessels. Thus, it is an aim of this work to understand the influence of the gel volume in an autoclave on the physicochemical properties of MOR. Moreover, an effect of the silica sources, from acid leaching and precipitation, was studied.

Materials and Methods

Preparation of Rice Husk Silica by Reflux and Calcination

RH was obtained from a local mill near Suranaree University of Technology, Thailand. It was washed several times with tap water, soaked in deionized (DI) water for 10 min and dried at 70°C overnight. Twenty five grams of the dried RH was put into a 250-mL round bottom flask, 180 mL of 3 M HCl solution (prepared from 37% HCl, Merck & Co., Inc., White House Station, NJ, USA) was added, and it was acid treated at 100°C for 6 h. The acid treated RH was washed several times with tap water until the pH of the wash solution was equal to that of the tap water, and it was then soaked in DI water for 10 min, dried at 70°C overnight, and calcined at 600°C for 6 h in a muffle furnace (Carbolite Ltd., Hope Valley, UK) with a heating rate of 2°C/min.

Preparation of Rice Husk Silica by Dissolution-Precipitation

First, RHA was prepared by calcination of the dried RH at 600°C in the muffle furnace with a heating rate of 2°C/min and cooled to room temperature. Four grams of RHA was dissolved in a 100 mL NaOH solution (prepared from NaOH pellets (Merck) with an RHA: NaOH weight ratio of 1:1.9) in a polyethylene bottle under magnetic stirring with a speed of 300 rpm for 36 h at room temperature. Then, the solution was filtered through a filter paper (Whatman No.1, Sigma-Aldrich Co., LLC, St. Louis, MI, USA) by an aspirator to a polyethylene beaker, to which was added a 6 N H_2SO_4 solution (Sigma- Aldrich) dropwise from a burette until the pH was about 11. Then, the solution was heated to 90-95°C with the continuous addition of sulfuric acid. Precipitation of the silica began when the pH was about 10.5-10.6. Then, DI water (50 mL) was added and the gel was broken by magnetic stirring. The H_2SO_4 solution was further added until the pH was 7 and the mixture was kept under stirring at this condition for 3 h. The precipitated silica was separated by centrifugation and washed repeatedly with warm DI water until the pH of the washed water was equal to that of the DI water. Then, the precipitated silica powder was dried at 120°C for 24 h in a hot air oven.

Synthesis of Mordenite (MOR)

The NaMOR was synthesized with a procedure adapted from Kim and Ahn (1991). Silica (either refluxed RHS or precipitated RHA) was suspended in DI water to form a slurry in a polypropylene bottle. Then, sodium aluminate (Riedel-de Haën AG Seelze, Germany, 41.383% Na_2O, 58.604% Al_2O_3) in NaOH solution was added under a magnetic stirring (250 rpm) at room temperature to produce a gel with the following molar ratio: $6Na_2O$:Al_2O_3:$29.2SiO_2$:$780H_2O$. The mixture was transferred to a Teflon-lined stainless steel autoclave and crystallized at 170°C (with a heating rate of 2.5ºC/min) without agitation for 120 h. The autoclave volume was 250 mL and the percent of gel/autoclave volume was 30, 50, and 70%. The sample was named according to the silica type and gel volume. For example, R-MOR-30 was the product from acid treated RHS with a volume 30% of the autoclave volume; P-MOR-70 was the product from precipitated RHS with a volume 70% of the autoclave volume. After crystallization, the product was separated by centrifugation, washed thoroughly with DI water, and dried at 100°C overnight.

Characterization

The phase of NaMOR was studied with X-ray diffraction (XRD) using a Bruker AXS D5005 (Bruker Corp., Billerica, MA, USA) with nickel-filtered Cu Kα radiation (wavelength = 1.54 Å) scanning in the 2θ range of 5–50°, at an increment of 0.02° and scan speed of 1 s/step. The elemental analysis was determined by X-ray fluorescence (XRF) using a Horiba Scientific XGT-5200 (Horiba Ltd., Kyoto, Japan). Morphologies of the silica were studied by scanning electron microscopy (SEM) using a JEOL/JSM-6010LV (JEOL Ltd., Tokyo, Japan). All samples were coated with gold by sputtering (Neocoater/mp-19020NCTR, JEOL Ltd.).

The N_2 adsorption-desorption isotherm of the NaMOR was obtained from a Micromeritics ASAP 2010 (Micromeritics Instrument Corp., Norcross, GA, USA). The surface area was determined using the Brunauer-Emmett-Teller (BET) method in a relative pressure range of 0.01–0.2. Each sample was first degassed at 300°C and the analysis was carried out at liquid nitrogen temperature.

The acidity of the NaMOR was determined by temperature-programmed desorption of ammonia (NH_3-TPD) in a Belcat-B (BEL Japan Inc., Osaka, Japan) equipped with a thermal conductivity detector. A sample amount of 250 mg was packed in a tubular U-shaped quartz cell, preheated at 500°C with a heating rate of 10°C/min in a He flow (50 mL/min) for 110 min to eliminate physisorbed species, and cooled to 70°C. Then a constant flow of 30 mL/min of 5 vol. % NH_3/Ar gas mixture was introduced over the samples for 30 min to achieve saturation. After purging with He for 5 min to remove physisorbed NH_3, the sample was heated to 130 °C with a heating rate of 10°C/min and held for 3 h to remove physisorbed species. The NH_3-TPD measurement was performed from 130 to 850°C with a heating rate of 10°C/min with He as a carrier gas. The number of acid sites was calculated from the peak area compared to a reference material with a known number of acid sites (ZSM-5) that was analyzed with the same conditions.

Results and Discussion

The XRD pattern of the obtained products from the acid treated RH silica, including R-MOR-30, R-MOR-50, and R-MOR-70, are shown in Figure 1. The pattern of all samples contained peaks with similar positions to those of the NaMOR reported in the literature (Mignoni *et al*., 2008; Zhang *et al*., 2009; Kulawong *et al*., 2011). However, samples with a different gel volume exhibited different intensity patterns. From R-MOR-30, the strongest peak was 9.8º followed by 25.7° corresponding to the planes 200 and 202, respectively. From R-MOR-50, the order of relative intensity was similar but the second peak became stronger. From R-MOR-70, a switch in the intensity order was observed. The growth of zeolite crystal depends on the solubility of the starting material and equilibrium within the autoclave during crystallization. The larger volume of the gel led to the higher autogeneous pressure in the autoclave and resulted in the higher solubility of the starting material. The crystal growth in the plane 202 from the reflux RHS increased with the gel volume. Kulawong *et al*. (2011) reported that NaMOR synthesized with an autoclave with a 150 mL capacity showed the strongest XRD peak at 25.6°. When the synthesis was carried out with an autoclave with a 250 mL capacity, the peak at 9.8° was the dominant one.

The XRD pattern of the obtained products from precipitated RH silica, including P-MOR-30, P-MOR-50, and P-MOR-70, are illustrated in Figure 2. The patterns of all samples also contain characteristic peaks of NaMOR (Mignoni *et al.*, 2008; Zhang *et al.*, 2009; Kulawong *et al.*, 2011) with the strongest peak from the plane 202. The intensity of the plane 200 increased with the gel volume. From P-MOR-50 and P-MOR-70, the intensity of the peak at 6.5° (corresponding to the plane 110) was significantly higher than that from P-MOR-50. The difference of peak intensity implied that the orientation of the NaMOR crystal from each batch was different. For example, it was reported by the Structure Commission of the International Zeolite Association that the intensity of the plane 200 was the highest in NaMOR with an Si/Al ratio of 5 (Baerlocher and McCusker, 2007).

The Si/Al mole ratios of all samples determined by XRF are listed in Table 1. The ratio in the product from both silica sources was higher than that in the gel. The Si/Al mole ratio of the NaMOR from the acid treated RHS

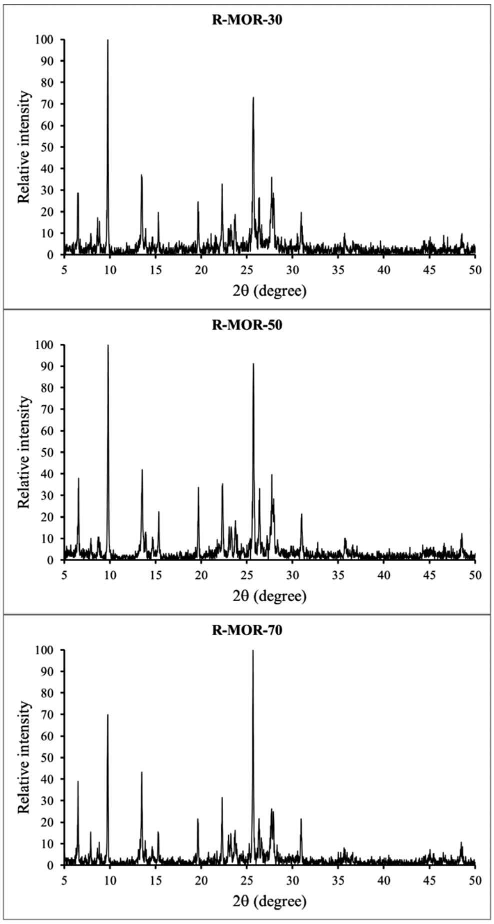

Figure 1. XRD patterns of NaMOR synthesized from acid treated rice husk silica with a gel volume of 30, 50, and 70% of the autoclave

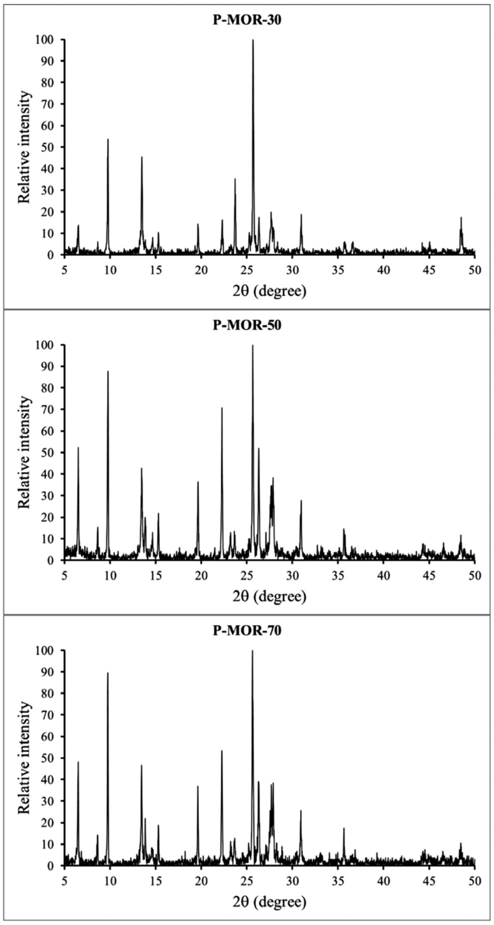

Figure 2. XRD patterns of NaMOR synthesized from precipitated rice husk ash with a gel volume of 30, 50, and 70% of the autoclave

increased with the gel volume. This result could be from the higher solubility of RHS for the sample with the higher gel volume. In the case of the NaMOR from precipitated RHA, the change in the Si/Al mole ratio could not be related to the gel volume. The lowest Si/Al mole ratio was from P-MOR-50. From observation, the silica from precipitation could be dissolved more easily than the acid treated RHS.

The N_2 adsorption-desorption isotherms of the NaMOR are presented in Figure 3. The isotherm of all samples was type I, according to the International Union of Pure and Applied Chemistry classification, which is the

Table 1. Si/Al ratios and surface areas of the synthesized MOR

Sample	Method to obtain rice husk silica	% Gel volume in autoclave	Gel Si/Al	Product Si/Al	BET surface area (m^2/g)
R-MOR-30	Reflux	30	14.6	57.6	215
R-MOR-50	Reflux	50	14.6	62.2	357
R-MOR-70	Reflux	70	14.6	65.2	347
P-MOR-30	Precipitation	30	14.6	56.1	435
P-MOR-50	Precipitation	50	14.6	48.1	432
P-MOR-70	Precipitation	70	14.6	49.3	418

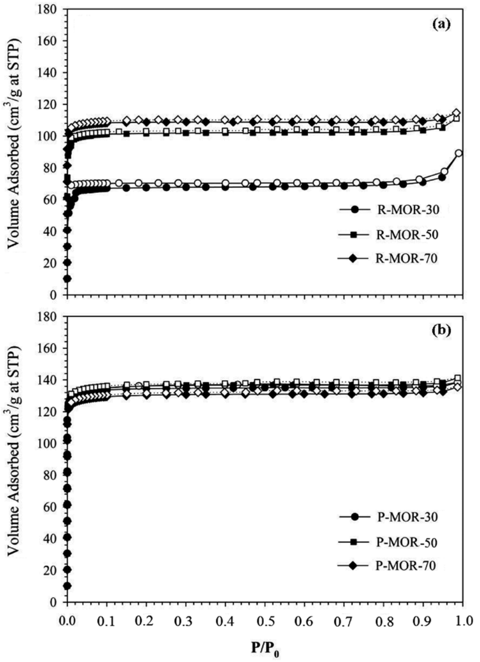

Figure 3. **N_2 adsorption–desorption isotherm of NaMOR synthesized with a gel volume of 30, 50, and 70% of the autoclave by using (a) acid treated rice husk silica and (b) precipitated rice husk ash**

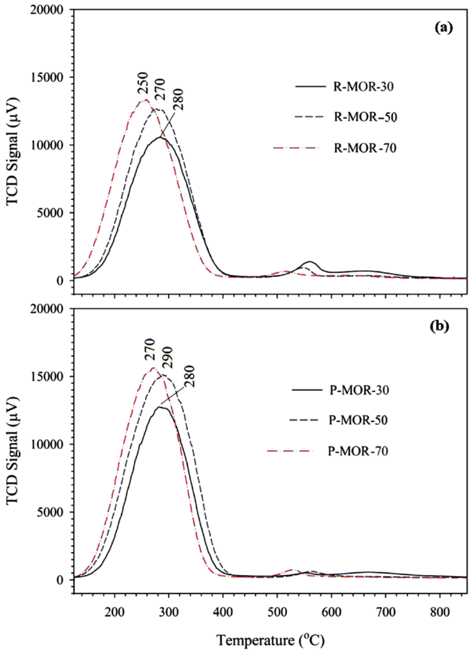

Figure 4. **NH_3-TPD profile of NaMOR synthesized with a gel volume of 30, 50, and 70% of the autoclave by using (a) acid treated rice husk silica and (b) precipitated rice husk ash**

characteristic of microporous materials. The adsorption increased rapidly at a low relative pressure corresponding to the adsorption in micropores and became nearly constant afterwards. The BET surface areas are included in Table 1. The surface area of the NaMOR synthesized with the acid treated RHS increased with the gel volume. The surface area of R-MOR-30 was significantly lower than R-MOR-50 and R-MOR-70 implying that R-MOR-30 had lower uniformity. This could be an effect from a lower pressure in the autoclave which resulted in a lower solubility of the RHS. In contrast, the surface areas of the NaMOR prepared from the precipitated RHA were close to each other. This result may due to the better solubility of the precipitated RHA.

The NH_3-TPD profiles of the NaMOR synthesized with different volumes are shown in Figure 4. All the NaMOR exhibited a large peak at lower than 400°C and a small peak at higher than 500°C, similar to the results from the literature (Katada *et al*., 2004; Kulawong *et al*., 2011). The low and high temperature peaks corresponded to the ammonia desorbed from the Brønsted and Lewis acid sites, respectively (Karge and Dondur, 1990; Ma *et al*., 2000). The peak area of the NaMOR from both silica sources increased with the gel volume (Table 2). The desorption temperatures of R-MOR-30 and P-MOR-30 were lower than those of other samples corresponding to the weaker acid sites. Ma *et al*. (2000) proposed that the ammonia desorption from ZSM-5 at low temperature was associated with the ammonia adsorbed either on Si–OH or from non-zeolitic impurity. The peak desorbed at high temperature was related to the ammonia adsorbed on Si–OH–Al.

The SEM micrographs of the NaMOR synthesized from acid treated and precipitated RHS are illustrated in Figures 5 and 6, respectively. Particles of the NaMOR synthesized from acid treated RHS (Figure 5) were not uniform in size and shape. Aggregated plate-like sheets and amorphous-like matter were observed. Particles of the NaMOR synthesized from precipitated RHS (Figure 6) were more uniform with less amorphous-like matter. The particle size decreased with the gel volume in the autoclave. The larger crystal size related to the fewer nuclei formed in the synthesis gel (Cundy and Cox, 2005; Cubillas and Anderson, 2010). Moreover, the uniformity of the zeolite crystal synthesized by using the hydrothermal method was crucially related to the homogeneous distribution of the starting nuclei in the system (Mintova and Valtchev, 2002).

Conclusions

NaMOR was synthesized by the hydrothermal method using acid treated RHS and precipitated RHA. All products exhibited characteristic XRD peaks of MOR with different intensity patterns. With an increase of the starting gel in the autoclave, the strongest peak in the NaMOR

Table 2. NH3-TPD peak position and acidity of NaMOR

Sample	Low temperature peak		High temperature peak	
	Peak position (°C)	Acidity (mmol/g)	Peak position	Acidity (mmol/g)
R-MOR-30	280	0.884	560	0.098
R-MOR-50	270	1.071	550	0.058
R-MOR-70	250	1.223	510	0.071
P-MOR-30	282	1.017	550	0.060
P-MOR-50	290	1.364	560	0.027
P-MOR-70	270	1.376	530	0.028

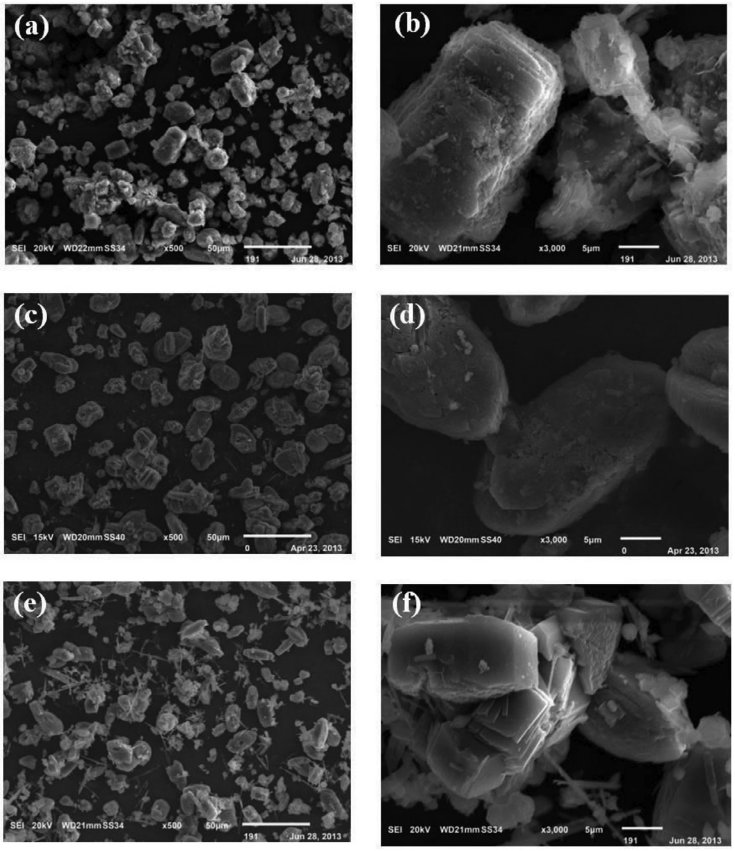

Figure 5. SEM images of NaMOR synthesized from acid treated rice husk silica with a gel volume of 30, 50, and 70 % of the autoclave (a) R-MOR-30 (low magnification) (b) R-MOR-30 (high magnification) (c) R-MOR-50 (low magnification) (d) R-MOR-50 (high magnification) (e) R-MOR-70 (low magnification) (f) R-MOR-70 (high magnification)

from acid treated RHS changed from plane 200 to 202. On the other hand, the strongest peak in the NaMOR from precipitated RHA was from the plane 202. In the NaMOR from acid treated RHS, the Si/Al mole ratio, surface area, and Bronsted acidity increased with the gel volume. In the NaMOR from precipitated RHA, the connection between either the Si/Al ratio or the surface area and the gel volume could not be made. However, the Bronsted acidity increased with the gel volume. The NaMOR from the precipitated RHS had a higher surface area and uniformity in the particle shape and size than that from the acid treated RHS.

Acknowledgements

The scholarship for S. Rakmae was from the Royal Golden Jubilee Ph.D program from the Thailand Research Fund (TRF) and Suranaree University of Technology (Grant No. PHD/0173/2553).

References

Artkla, S., Grisdanurak, N., Neramittagapong, S., and Wittayakun, J. (2008). Characterization and catalytic performance on transesterification of palm olein of potassium oxide supported on RH-MCM-41 from rice husk silica. Suranaree J. Sci. Technol., 15(2):133-138.

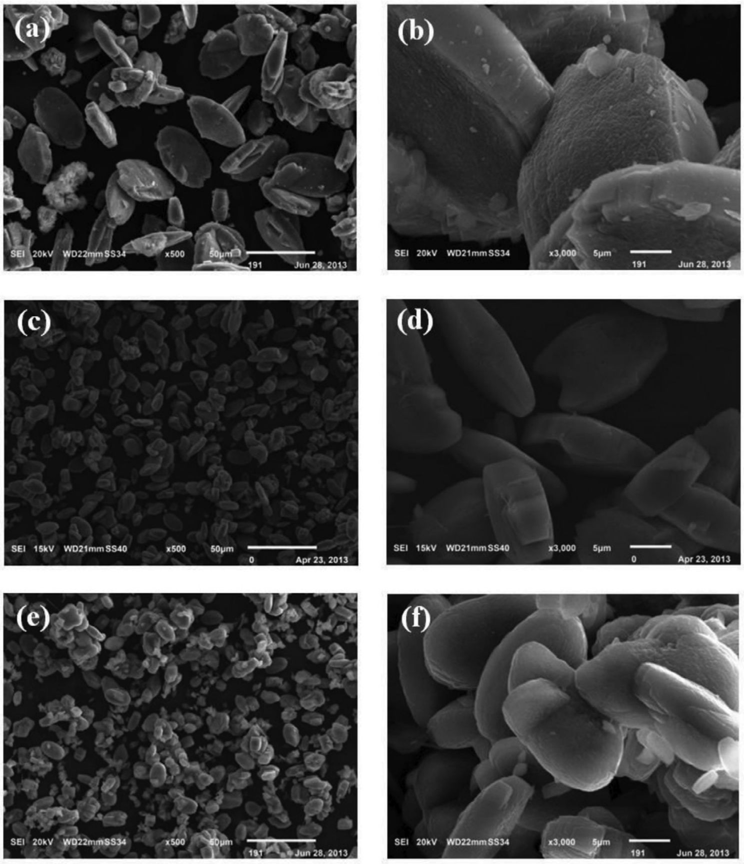

Figure 6. SEM images of NaMOR synthesized from precipitated rice husk ash with a gel volume of 30, 50, and 70 % of the autoclave (a) P-MOR-30 (low magnification) (b) P-MOR-30 (high magnification) (c) P-MOR-50 (low magnification) (d) P-MOR-50 (high magnification) (e) P-MOR-70 (low magnification) (f) P-MOR-70 (high magnification)

Baerlocher, C. and McCusker, L.B. (2007). Database of Zeolite Structures. Newark, DE, USA: International Zeolite Association. Available from: http://www.iza-structure.org/databases/.

Cubillas, P. and Anderson, M.W. (2010). Pore structure, diffusion and activity at the subcrystal level. In: Zeolites and Catalysis. Cejka, J., Corma, A., and Zones, S., (eds). Wiley-VCH Verlag GmbH, Weinheim, Germany, p. 375-379.

Cundy, C.S. and Cox, P.A. (2005). The hydrothermal synthesis of zeolites: Precursors, intermediates and reaction mechanism. Micropor. Mesopor. Mat., 82(1-2):1-78.

Juliano, B.O., Maniñgat, C.C., and Pascual, C.G. (1987). Properties of fraction of rice hull. Phytochemistry, 26(12):3261-3263.

Kalapathy, U., Proctor, A., and Shultz, J. (2000). A simple method for production of pure silica from rice hull ash. Bioresource Technol., 73(3):257-262.

Karge, H.G. and Dondur, V. (1990). Investigation of the distribution of acidity in zeolites by temperature-programmed desorption of probe molecules. I. Dealuminated mordenites. J. Phys. Chem., 94 (2):765-772.

Katada, N., Kanai, T., and Niwa, M. (2004). Dealumination of proton form mordenite with high aluminum content in atmosphere. Micropor. Mesopor. Mat., 75(1-2):61-67.

Khabuanchalad, S., Khemthong, P., Prayoonpokarach, S., and Wittayakun, J. (2008). Transformation of zeolite NaY synthesized from rice husk silica to NaP during hydrothermal synthesis. Suranaree J. Sci. Technol., 15(3):225-231.

Khemthong, P., Prayoonpokarach, S., and Wittayakun, J. (2007). Synthesis and characterization of zeolite LSX from rice husk silica. Suranaree J. Sci. Technol., 14(4):367-379.

Kim, G.J. and Ahn, W.S. (1991) Direct synthesis and characterization of high-SiO_2-content mordenites. Zeolites, 11(7):745-750.

Kordatos, K., Gavela, S., Ntziouni, A., Pistiolas, K.N., Kyritsi, A., and Kasselouri-Rigopoulou, V. (2008). Synthesis of highly siliceous ZSM-5 zeolite using silica from rice husk ash. Micropor. Mesopor. Mat., 115(1-2):189-196.

Krishnarao, R.V., Subrahmanyam, J., and Kumar, T.J. (2001). Studies on the formation of black particles in rice husk silica ash. J. Eur. Ceram. Soc., 21(1):99-104.

Kulawong, S., Prayoonpokaracha, S., Neramittagapong, A., and Wittayakun, J. (2011). Mordenite modification and utililization as supports for iron catalyst for phenol hydroxylation. J. Ind. Eng. Chem., 17(2):346-351.

Liou, T.H. (2004). Preparation and characterization of nano-structured silica from rice husk. Mater. Sci. Eng. A., 364(1-2):313-323.

Liou, T.H. and Yang, C.C. (2011). Synthesis and surface characteristics of nanosilica produced from alkali-extracted rice husk ash. Mater. Sci. Eng. B., 176(7):521-529.

Loiha, S., Föttinger, K., Zorn, K., Klysubun, W., Rupprechter, G., and Wittayakun, J. (2009). Catalytic enhancement of platinum supported on zeolite beta for toluene hydrogenation by addition of palladium. J. Ind. Eng. Chem., 15(6):819-823.

Ma, D., Zhang, W., Shu, Y., Liu, X., Xu, Y., and Bao, X. (2000). MAS NMR, ESR and TPD studies of Mo/HZSM-5 catalysts: evidence for the migration of molybdenum species into the zeolitic channels. Catal. Lett., 66(3):155-160.

Makornpan, M., Mongkolkachit, C., and Wasanapiarnpong, T. (2013). Fabrication of silicon carbide ceramics from rice husks. Suranaree J. Sci. Technol., 21(2):79-86.

Mao, R.L.V., Al-Yassir, N., Lu, L., Vu, N.T., and Fortier, A. (2006). New method for the study of surface acidity of zeolites by NH_3-TPD, using a pH-meter equipped with an ion selective electrode. Catal. Lett., 112(1-2):13-18.

Meier, W. M. (1961). The crystal structure of mordenite (ptilolite). Z. Kristallogr., 115:439-450.

Mignoni, M.L., Petkowicz, D.I., Machado, N.R.C.F., and Pergher, S.B.C. (2008). Synthesis of mordenite using kaolin as Si and Al source. Appl. Clay Sci., 41(1-2):99-104.

Mintova, S. and Valtchev, V. (2002). Effect of the silica source on the formation of nanosized silicalite-1: an in situ dynamic light scattering study. Micropor. Mesopor. Mat., 55(2):171-179.

Naskar, M.K., Kundu, D., and Chatterjee, M. (2012). A facile hydrothermal conversion of rice husk ash to ZSM-5 zeolite powders. J. Am. Ceram. Soc., 95(3):925-930.

Panpa, W. and Jinawath, S. (2009). Synthesis of ZSM-5 zeolite and silicalite from rice husk ash. Appl. Catal. B-Environ., 90(3-4):389-394.

Pimsuta, M., Neramittagapong, A., Prayoonpokarach, S., and Wittayakun, J. (2012). Desilication of NaZSM-5 and utilization as support of Fe for phenol hydroxylation. International Journal of Chemical Engineering and Applications, 3(2):86-91.

Pantu, P., Boekfa, B., and Limtrakul, J. (2007). The adsorption of saturated and unsaturated hydrocarbons on nanostructured zeolites (H-MOR and H-FAU): An ONIOM study. J. Mol. Catal. A-Chem., 277(1-2):171-179.

Roland, E. and Kleinschmit, P. (2003). Zeolites. In: Ullmann's Encyclopedia of Industrial Chemistry. Vol.39. 6th ed. Bohnet, M. and Brinker, C. J., (eds). Wiley-VCH Verlag GmbH, Weinheim, Germany, p. 687-716.

Tepamat, T., Mongkolkachit, C., and Wasanapiarnpong, T. (2013). Synthesis of zeolite NaA and activated carbon composite from rice husk. Suranaree J. Sci. Technol., 21(2):119-123.

Wittayakun, J., Khemthong, P., and Prayoonpokarach, S. (2008). Synthesis and characterization of zeolite NaY from rice husk silica. Korean J. Chem. Eng., 25 (4):861-864.

Zhang, L., van Laak, A.N.C., de Jongh, P.E., and de Jong, K.P. (2009). Synthesis of large mordenite crystals with different aspect ratios. Micropor. Mesopor. Mat., 126(1-2):115-124.